TU Delft

Delft University of Technology

Licence
Dutch Copyright Act (Article 25fa)

Citation (APA)
Leibold, D., Goorden, M. C., & Schaart, D. R. (2026). Experimental Study on Dual-Energy Cone-Beam CT for Proton Therapy Planning. In A. Ganguly, K. Li, & S. Abbaszadeh (Eds.), *Medical Imaging 2026: Physics of Medical Imaging* Article 1392427 (Progress in Biomedical Optics and Imaging - Proceedings of SPIE; Vol. 13924). SPIE. https://doi.org/10.1117/12.3085612

Important note
To cite this publication, please use the final published version (if applicable).
Please check the document version above.

Copyright
In case the licence states “Dutch Copyright Act (Article 25fa)”, this publication was made available Green Open Access via the TU Delft Institutional Repository pursuant to Dutch Copyright Act (Article 25fa, the Taverne amendment). This provision does not affect copyright ownership.
Unless copyright is transferred by contract or statute, it remains with the copyright holder.

Sharing and reuse
Other than for strictly personal use, it is not permitted to download, forward or distribute the text or part of it, without the consent of the author(s) and/or copyright holder(s), unless the work is under an open content license such as Creative Commons.

Takedown policy
Please contact us and provide details if you believe this document breaches copyrights.
We will remove access to the work immediately and investigate your claim.

This work is downloaded from Delft University of Technology.

Experimental Study on Dual-Energy Cone-Beam CT for Proton Therapy Planning

David Leibold[a], Marlies C. Goorden[a], and Dennis R. Schaart[a,b]

[a]Department of Radiation Science and Technology, Delft University of Technology, Mekelweg 15, Delft, The Netherlands
[b]Holland Proton Therapy Center, Huismansingel 4, Delft, The Netherlands

ABSTRACT

The objective of this study is to test the ability of dual-energy CBCT to extract proton stopping power ratio (SPR) values for proton radiotherapy planning and to compare its performance to single-energy CBCT, while optimising the operating parameters of both single- and dual-energy CBCT for SPR extraction. We scanned three phantoms with a clinical CBCT installed in the gantry of a proton therapy facility at different source voltage and current settings. Dual-energy CBCT was emulated by combining scans from different kVps. We employed the Hünemohr-Saito method to predict SPR values for dual-energy CBCT scans, whereas we used a Hounsfield look-up table for predicting SPR values based on single-energy CT scans. The optimum operating parameters for dual-energy CBCT scans were an 80/125 kVp combination with a low/high kVp dose ratio of 75/25. This resulted in a relative mean error (RME) and a relative root mean square error (RRMSE) of $(0.1 \pm 1.2)\,\%$ and $(2.53 \pm 0.73)\,\%$, respectively. For single-energy CBCT scans, 125 kVp was determined to be the optimum voltage, yielding a RME and RRMSE value of $(1.5 \pm 3.3)\,\%$ and $(7.1 \pm 6.9)\,\%$, respectively. Although limited in scope and in need of further experiments, this study indicates that dual-energy CBCT performs better than single-energy CBCT.

Keywords: Cone-Beam CT, Stopping Power Ratio Prediction, Proton Therapy Planning, Proton Radiotherapy, Dual-Energy.

1. INTRODUCTION

Proton radiotherapy is being investigated as a promising form of radiotherapy.[1] The state-of-the-art imaging modality for extracting proton stopping power ratio (SPR) values for treatment planning is fan-beam CT.[2] Cone-beam CT (CBCT) is not used for treatment planning directly, but mostly as an in-room modality for patient positioning,[3,4] because its image quality is inferior to that of fan-beam CT due to scatter[5] and increased patient motion. In contrast to fan-beam CT, however, CBCT offers the possibility to integrate the imaging modality isocentrically with the proton beam. A possible route to enable direct utilisation of CBCT images in treatment planning could be to enhance CBCT setups in such a way that they can extract spectral information from X-rays. This hypothesis is based on previous studies that have shown that better accuracy and robustness can be achieved when using spectral fan-beam CT instead of single-energy (SE) fan-beam CT.[6–14]

In a previous study we compared different dual-energy (DE) CBCT setups in silico,[15] which showed that, for realistic detectors, a kVp-switching setup with energy-integrating detectors performs best. The aim of this study was hence to investigate the performance of DE CBCT with a clinical system, emulating a kVp-switching setup, and to compare the accuracy and robustness of SPR extraction from (emulated) DE CBCT scans and SE CBCT scans. We emulated DE CBCT scans by scanning three different phantoms subsequently at different source voltages, and tested different combinations of low- and high-energy source voltages, as well as different ratios of dose assigned to the low and high energy scans. Similarly, we tested different source voltages for SE CBCT. The total dose was kept the same for all DE and SE scans. We applied the Hünemohr-Saito (HS) method and a Hounsfield look-up table (HLUT) for predicting SPRs based on DE and SE scans, respectively.

Further author information: Send correspondence to D.R.S.
E-mail: d.r.schaart@tudelft.nl

Medical Imaging 2026: Physics of Medical Imaging, edited by Ke Li, Shiva Abbaszadeh, Arundhuti Ganguly,
Proc. of SPIE Vol. 13924, 1392427 · 2026 Published by SPIE
1605-7422 · doi: 10.1117/12.3085612

2. METHODOLOGY

2.1 Acquisition of CBCT Scans

We scanned a Catphan 700 phantom (diameter of 200 mm; The Phantom Laboratory), a CIRS 062 Electron Density phantom (diameter of 180 mm; Sun Nuclear Corp.), and a Gammex 467 phantom (diameter of 330 mm; the outer ring of inserts is arranged along a circle with 220 mm diameter; Sun Nuclear Corp.). We calculate values for the relative electron density ($\rho_{\text{elec}}^{\text{rel}}$), the effective atomic number (Z_{eff}), and the SPR based on elemental composition and physical mass density data of nominal values provided by the manufacturers, with the exception of the physical mass density of inserts of the Gammex and CIRS phantom, for which specific physical mass density values are available. For details on the calculation of $\rho_{\text{elec}}^{\text{rel}}$, Z_{eff} and SPR we refer to our previous work in Ref. 15.

CBCT scans were acquired in a proton therapy treatment gantry (Varian ProBeam System, Varian Medical Systems, Inc., Palo Alto, CA) of the Holland Proton Therapy Center (HollandPTC). The phantoms were scanned with the three available X-ray source voltages of 80 kVp, 100 kVp, and 125 kVp. For a fair comparison between different combinations of scans with different voltages, we kept the total radiation output by the system the same for all combinations. Specifically, scans were acquired with source currents of 100 %, 75 %, 50 % and 25 % of the maximum radiation output. We then combined scans from different voltages such that the total radiation output always equaled 100% of the maximum dose. The resulting DE SPR predictions were then compared to SE scans acquired at 100 % of the maximum dose.

All scans were reconstructed with the default reconstruction software available on the clinical system. The three available kVp voltages could only be used in a mode that is intended for head scans, featuring a limited field-of-view (FOV) with a diameter of 289.5 mm. The Gammex phantom's body is wider than this FOV, which in principle gives rise to severe reconstruction artefacts. However, its inserts protrude from the phantom body and still fit inside the field of view. We therefore used the reconstructed slices without the Gammex phantom body for evaluation.

2.2 Proton Stopping Power Ratio Prediction

We follow the conventional approach of using a Hounsfield look-up table (HLUT) to predict SPR values from SE CBCT scans. For details on the process of specifying a HLUT we refer the reader to the consensus guide by Peters, Taasti et al[16] whose reference implementation was adapted for this study.

We implemented the Hünemohr-Saito (HS) method introduced by Li et al[17] to predict SPR values from DE CBCT scans. This method assumes a linear relationship between $\rho_{\text{elec}}^{\text{rel}}$ and the so-called *subtracted CT number*, which is a linear combination of the Hounsfield (HU) values obtained at low and high energy. Analogously, it assumed that there is a linear relationship between the product of $\rho_{\text{elec}}^{\text{rel}} \cdot Z_{\text{eff}}^{n}$ (with n being set to 3.1) and a dedicated subtracted CT number. In order to convert the effective atomic number to an ionisation energy, we apply the approach by Yang et al[14] which assumes a linear relation between Z_{eff} and the logarithm of the ionisation energy, $\ln(I)$.

When applying the HS method to obtain SPR values, it is possible that a negative value for $\rho_{\text{elec}} \cdot Z_{\text{eff}}^{n}$ is predicted, in which case taking the n^{th} root to obtain Z_{eff} yields a non-physical complex value. This occurred for the following phantom inserts for at least one set of parameters: Catphan phantom: 'Lung foam' and 'polystyrene'; CIRS phantom: 'Lung (inhale)'; Gammex phantom: 'LN300 lung'. These four inserts, along with the Catphan inserts 'air hole' and its empty vial, are excluded from evaluation when comparing the results for different source voltage combinations and dose ratios. In order to make the HS and the HLUT method as comparable as possible, the same inserts were excluded from evaluation in both the HLUT and HS approach.

2.3 Error Metrics

In the following, we describe the error metrics used within this work to evaluate SPR values.

The relative mean error (RME) quantifies the bias and is defined as

$$\text{RME} = \frac{1}{N} \sum_i \frac{\Delta x_i}{x_{\text{gt},\,i}} = \frac{1}{N} \sum_i \frac{x_{\text{gt},\,i} - x_{\text{p},\,i}}{x_{\text{gt},\,i}} \quad , \qquad (1)$$

with $x_{\text{gt},\,i}$ as the ground truth value of insert i, $x_{\text{p},\,i}$ as the predicted value of insert i, and Δx_i as the difference between these two values. Note that for ground truth values on SPR, $x_{\text{gt}} > 0$ always holds, with $x_{\text{gt}} \in [0.178, 1.80]$.

The relative root mean square error (RRMSE) is defined as

$$\text{RRMSE} = \frac{\sqrt{\frac{1}{N} \sum_i (x_{\text{gt},\,i} - x_{\text{p},\,i})^2}}{\frac{1}{N} \sum_i x_{\text{gt},\,i}} \quad . \qquad (2)$$

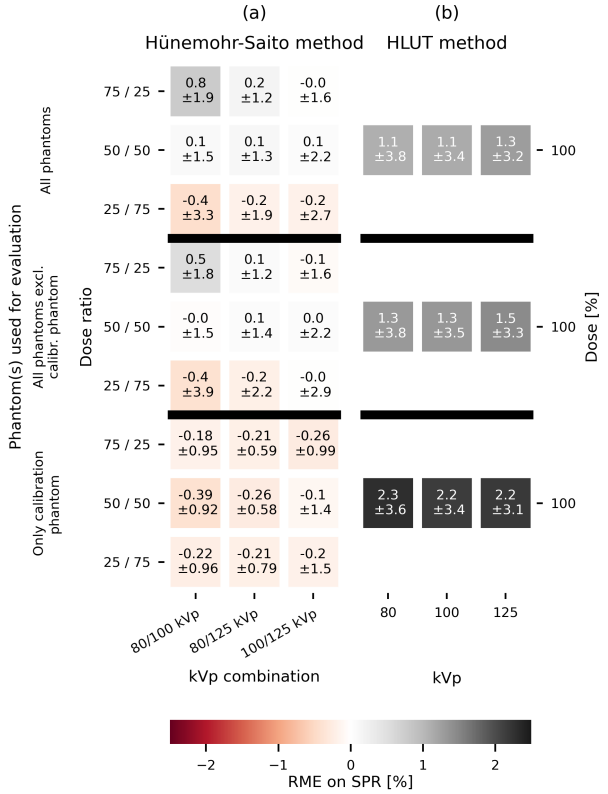


Figure 1. RME on SPR for (a) dual-energy CBCT and (b) single-energy CBCT. The results are grouped according to the phantom(s) used for evaluation: the same phantom that was used for calibration (bottom row), all phantoms except the calibration phantom (centre row), or all phantoms (top row). The dose ratio is given as the ratio between the dose given to the low and high energy scan.

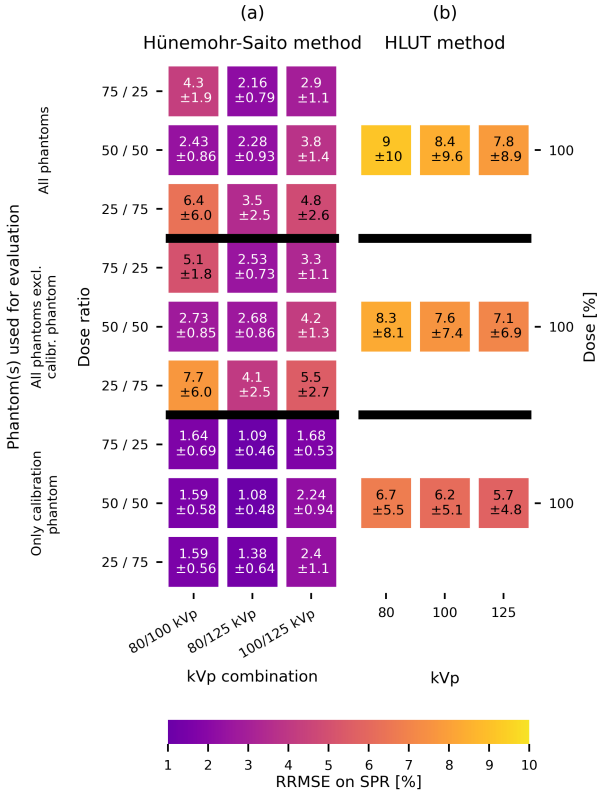


Figure 2. RRMSE on SPR for (a) dual-energy CBCT and (b) single-energy CBCT. The results are grouped by according to the phantom(s) used for evaluation: the same phantom that was used for calibration (bottom row), all phantoms except the calibration phantom (centre row), or all phantoms (top row). The dose ratio is given as the ratio between the dose given to the low and high energy scan.

3. RESULTS

For both the HS and the HLUT method we use three different scenarios to evaluate SPR prediction performance: we use one phantom for calibration, while for evaluation we use either (1) the same phantom, (2) all but the calibration phantom, or (3) all three phantoms (including the calibration phantom). While we obtained results separately for each of the three possible choices for the calibration phantom and for each of the three aforementioned scenarios, for conciseness we report here the mean values of RME and RRMSE taken over all three choices of calibration phantom.

We would like to point out that scenario (2), evaluated for all choices of a calibration phantom, results in a leave-one-out cross validation, which makes it the scenario that is the most indicative of how well the applied SPR extraction method is able to generalise, under the constraints of using similar phantom diameter, insert compositions, and scan settings. For this reason, while we will also show results on scenarios (1) and (3) in the referenced figures and tables, we focus mainly on scenario (2).

For the HLUT method applied to SE CBCT scans, we show results for each choice of kVp; the dose is always kept at 100 % to enable a fair comparison with DE scans. Figures 1b and 2b show the RME and RRMSE for the three scenarios used for evaluation (only calibration phantom, all phantoms except calibration phantom, and all phantoms), averaged over all three possible calibration phantoms.

The centre row in Figure 1b (all phantoms used for evaluating SPR prediction bias except the calibration phantom) shows that the lowest RME value of 1.3 % is achieved for source voltages of either 80 or 100 kVp. The difference in RME compared to 125 kVp, however, is small (a factor of 1.1).

Examining the results achieved by applying a HLUT in terms of RRMSE (Figure 2b), we find that this metric is lowest for a 125 kVp source voltage, with a RRMSE of (7.1 ± 6.9) %. The minimum and maximum values achieved for different choices of the source voltage differ by a factor of 1.2.

For the HS method applied to DE CBCT scans, we show results for each chosen kVp combination as well as for each dose ratio. Figures 1a and 2a show RME and RRMSE for the three scenarios used for evaluation (only calibration phantom, all phantoms except calibration phantom, and all phantoms), averaged over all three possible calibration phantoms.

The centre row in Figure 1a (all phantoms used for evaluating SPR prediction bias except the calibration phantom) shows that the lowest RME value, i.e., the smallest bias, is achieved in several instances: a 100/125 kVp voltage combination and either a 25/75 dose ratio (25 % of the dose assigned to the low energy scan, 75 % to the high energy scan) or a 50/50 dose ratio, and an 80/100 kVp voltage combination and a 50/50 dose ratio, all resulting in a RME of 0.0 (within the given uncertainty).

Examining the results achieved by the HS method in terms of RRMSE (Figure 2a), we find that this metric is lowest for an 80/125 kVp combination and a 75/25 dose ratio, with a RRMSE of (2.53 ± 0.73) %. For this set of optimum parameters, the RME is still low compared to other choices of operating parameters, with a value of RME = (0.1 ± 1.2) %. The minimum and maximum values achieved for different choices of operating parameters differ by a factor of 3.0 for the error metric of RRMSE.

4. DISCUSSION

Comparing the performance of SPR extraction based on DE CBCT scans with the HS method to that based on SE CBCT scans applying a HLUT, we find that in terms of bias, the HS method achieves a minimum RME of (0.0 ± 2.9) %, whereas the HLUT achieves a best value of (1.3 ± 3.8)%, the difference being about two orders of magnitude difference. In terms of RRMSE, they achieve values of (2.53 ± 0.73) % and (7.1 ± 6.9), respectively, which differ by a factor of about 2.8. As a result, the HS method outperforms the HLUT-based method in both error metrics in this study.

However, additional research will be needed before definite conclusions can be drawn about the performance of SE and DE CBCT for SPR extraction, as this first study still has several limitations. First, differences in HU units due to different phantom sizes or even an absent phantom body, resulting in a varying degree of beam hardening correction. Second, inserts with different material classes being used for either calibration or evaluation. Third, relatively small phantom sizes, limiting the amount of scatter and hence mitigating the most influential detrimental effect to image quality in CBCT.

To address the first point of different phantom sizes or even an absent phantom body, we evaluated the RME and RRMSE for each phantom separately. We find that in most cases, using the Gammex phantom for calibration and applying it to other phantoms, or using either the Catphan or CIRS phantom for calibration and applying these to the Gammex phantom, yields the largest RRMSE values. We attribute this to the fact that only slices without the Gammex phantom's body are used, which leads to an over-correction by the beam hardening correction algorithm.

Concerning the second point of different material classes of inserts, we would like to point out that the CIRS and Gammex phantom only exhibit inserts designed to to mimic human-like tissues. In contrast, the Catphan phantom exhibits only three human tissue-like materials, whereas its other inserts are commercially available plastics.

Third, since we were able to use only a smaller field of view with our scanner and hence phantoms comparable to human head size, the conclusions in this work apply only to objects with a similar diameter. Although tumors in the head and neck region are among the main indications for proton therapy, larger phantoms introduce more severe scatter, which is one of the main reasons for the inferior image quality of CBCT when compared to fan-beam CT. The influence of larger diameters of the object under investigation is therefore yet to be determined.

While a number of studies have been published comparing DE fan-beam CT (DECT) to SE fan-beam CT (SECT), it is often difficult to directly compare these to the present work due to differences in the study design. A notable exception is the work by Moskvin et al,[8] who evaluated both SE and DE SPR estimation algorithms using a dual-layer fan-beam CT and a Gammex 467 phantom for both calibration as well as evaluation. Based on their published data, we calculate a RME of -1.8 % (0.14 %) and a RRMSE of 2.2 % (0.65 %) for SECT (DECT). In our case, the best values achieved when using the Gammex phantom for both calibration and evaluation are a RME of -0.36 % (0.21 %) and a RRMSE error of 1.60 % (0.93 %) for SE CBCT (DE CBCT). Hence, our results obtained via SE CBCT are

consistently better than those reported by Moskvin et al for SE fan-beam CT, which is unexpected due to the generally worse image quality of CBCT compared to fan-beam CT. For DE CBCT, our results are consistently worse compared to Moskvin et al, which aligns with our expectations for the same reason. The unexpected findings in case of SE acquisitions could be due to the fact that Moskvin et al also used their dual-layer detector for acquiring SE images or due to different HLUT implementations, and requires a more thorough analysis.

5. CONCLUSION

We investigated the use of dual-energy cone-beam CT for extraction of proton stopping power ratios for proton therapy planning. We emulated a dual-energy CBCT setup by sequentially scanning three phantoms at different tube voltages. SPR values were extracted using the Hünemohr-Saito method, and compared to SPR values extracted from single-energy scans using a Hounsfield look-up table. We find that DE CBCT consistently performed better in this study. However, we also discuss the limitations of this study, which warrant further research before definitive conclusions can be drawn about the performance of SE and DE CBCT for SPR extraction.

Disclosures

D.L. is funded by Varian Medical Systems, Inc., A Siemens Healthineers Company, grant number 2018016. M.C.G. and D.R.S. have nothing relevant to disclose.

Disclaimer

This work is not being and has not been submitted for publication or presentation elsewhere.

ACKNOWLEDGMENTS

A large number of people was involved in the planning and execution of this study, all of whom made this research possible. We would therefore like to express our sincere gratitude to everyone, and we appreciate all the generous help and support we received.

More specifically, we would like to thank the staff at HollandPTC for supporting us in both technical and operational manner (in alphabetical order): Astrid Moerman, Charlotte van der Vos, Hansjoerg Wertz, Mischa Hoogeman, Patricia Lopes, Paola Flores Sanchez, Paul van Beers, and Rob Louwe. A special thanks goes to Henry Noordmans and Vera Schroen for performing the CBCT scans for us. Furthermore, we would like to thank the staff at Varian who was always readily answering our technical questions (in alphabetical order): Adam Harrington, Erik Visser, Mitchel Low, Radek Ofierzynski, Roberto Cassetta, Vladimir Balaz, and the on-site Varian engineers at HPTC. Furthermore, we would like to thank the staff at Erasmus MC for their support (in alphabetical order): Marcel van Straaten, Michelle Oud, Miriam Both, Paulette Prins, and Sophie Huijskens, Furthermore, we would like to thank Esther Plomp for her support and Lukas Schroeder for helpful discussions, and the staff at The Phantom Laboratory, manufacturer of the Catphan phantom, for their support. A special thank goes to Bob Duivestein, whose work[18] paved the way for this study.

Finally, we would like to thank Varian Medical Systems, Inc., A Siemens Healthineers Company, for their funding.

REFERENCES

[1] Chen, Z., Dominello, M. M., Joiner, M. C., and Burmeister, J. W., "Proton versus photon radiation therapy: A clinical review," *Frontiers in Oncology* **13**, 1133909 (Mar. 2023).

[2] Bolsi, A., Peroni, M., Amelio, D., Dasu, A., Stock, M., Toma-Dasu, I., Nyström, P. W., and Hoffmann, A., "Practice patterns of image guided particle therapy in Europe: A 2016 survey of the European Particle Therapy Network (EPTN)," *Radiotherapy and Oncology* **128**, 4–8 (July 2018).

[3] Landry, G. and Hua, C.-h., "Current state and future applications of radiological image guidance for particle therapy," *Medical Physics* **45** (Nov. 2018).

[4] Seco, J. and Spadea, M. F., "Imaging in particle therapy: State of the art and future perspective," *Acta Oncologica* **54**, 1254–1258 (Oct. 2015).

[5] Siewerdsen, J. H., Daly, M. J., Bakhtiar, B., Moseley, D. J., Richard, S., Keller, H., and Jaffray, D. A., "A simple, direct method for x-ray scatter estimation and correction in digital radiography and cone-beam CT: X-ray scatter correction," *Medical Physics* **33**, 187–197 (Dec. 2005).

[6] Bär, E., Lalonde, A., Royle, G., Lu, H.-M., and Bouchard, H., "The potential of dual-energy CT to reduce proton beam range uncertainties," *Medical Physics* **44**, 2332–2344 (June 2017).

[7] Möhler, C., Russ, T., Wohlfahrt, P., Elter, A., Runz, A., Richter, C., and Greilich, S., "Experimental verification of stopping-power prediction from single- and dual-energy computed tomography in biological tissues," *Physics in Medicine & Biology* **63**, 025001 (Jan. 2018).

[8] Moskvin, V. P., Pirlepesov, F., Yan, Y., Ates, O., Myers, W. J., Uh, J., Zhao, L., Shapira, N., Yagil, Y., Merchant, T. E., and Hua, C.-h., "Accuracy of stopping power ratio calculation and experimental validation of proton range with dual-layer computed tomography," *Acta Oncologica* **61**, 864–868 (July 2022).

[9] Peters, N., Wohlfahrt, P., Hofmann, C., Möhler, C., Menkel, S., Tschiche, M., Krause, M., Troost, E. G., Enghardt, W., and Richter, C., "Reduction of clinical safety margins in proton therapy enabled by the clinical implementation of dual-energy CT for direct stopping-power prediction," *Radiotherapy and Oncology* **166**, 71–78 (Jan. 2022).

[10] Taasti, V. T., Michalak, G. J., Hansen, D. C., Deisher, A. J., Kruse, J. J., Krauss, B., Muren, L. P., Petersen, J. B. B., and McCollough, C. H., "Validation of proton stopping power ratio estimation based on dual energy CT using fresh tissue samples," *Physics in Medicine & Biology* **63**, 015012 (Dec. 2017).

[11] Taasti, V. T., Muren, L. P., Jensen, K., Petersen, J. B. B., Thygesen, J., Tietze, A., Grau, C., and Hansen, D. C., "Comparison of single and dual energy CT for stopping power determination in proton therapy of head and neck cancer," *Physics and Imaging in Radiation Oncology* **6**, 14–19 (Apr. 2018).

[12] Wohlfahrt, P., Möhler, C., Richter, C., and Greilich, S., "Evaluation of Stopping-Power Prediction by Dual- and Single-Energy Computed Tomography in an Anthropomorphic Ground-Truth Phantom," *International Journal of Radiation Oncology*Biology*Physics* **100**, 244–253 (Jan. 2018).

[13] Xie, Y., Ainsley, C., Yin, L., Zou, W., McDonough, J., Solberg, T. D., Lin, A., and Teo, B.-K. K., "*Ex Vivo* validation of a stoichiometric dual energy CT proton stopping power ratio calibration," *Physics in Medicine & Biology* **63**, 055016 (Mar. 2018).

[14] Yang, M., Virshup, G., Clayton, J., Zhu, X. R., Mohan, R., and Dong, L., "Theoretical variance analysis of single- and dual-energy computed tomography methods for calculating proton stopping power ratios of biological tissues," *Physics in Medicine and Biology* **55**, 1343–1362 (Mar. 2010).

[15] Leibold, D., Schaart, D. R., and Goorden, M. C., "Optimising proton stopping power ratio prediction with spectral cone-beam CT," *Physics in Medicine & Biology* **70**, 145023 (July 2025).

[16] Peters, N., Trier Taasti, V., Ackermann, B., Bolsi, A., Vallhagen Dahlgren, C., Ellerbrock, M., Fracchiolla, F., Gomà, C., Góra, J., Cambraia Lopes, P., Rinaldi, I., Salvo, K., Sojat Tarp, I., Vai, A., Bortfeld, T., Lomax, A., Richter, C., and Wohlfahrt, P., "Consensus guide on CT-based prediction of stopping-power ratio using a Hounsfield look-up table for proton therapy," *Radiotherapy and Oncology* **184**, 109675 (July 2023).

[17] Li, B., Lee, H. C., Duan, X., Shen, C., Zhou, L., Jia, X., and Yang, M., "Comprehensive analysis of proton range uncertainties related to stopping-power-ratio estimation using dual-energy CT imaging," *Physics in Medicine & Biology* **62**, 7056–7074 (Aug. 2017).

[18] Duivestein, R. A., *Simulating and Evaluating Different Implementations of Dual Energy Cone-Beam CT for Proton Therapy Treatment Planning*, Master's thesis, Delft University of Technology, Delft (2024).